Dr.-Ing. Dierk Hobbie*
Carl Zeiss
Oberkochen, W. Germany

Orthophoto Project Planning

Focal length, photo scale, flight data, overlap percentages, design and type of flight, and instrumentation affect the eventual accuracy of the product.

In the course of the past few years, the method of differential rectification (orthophotography) has become increasingly popular. Its success is above all due to the higher production rate with which a product can be obtained whose accuracy and quality are comparable to those of a conventional map. However, the saving in time and, thus, the economy, accuracy and quality of that product, are not only determined by the instrumentation presently available but also to a large extent by the care used in planning and executing the project concerned.

Abstract: *It is the purpose of project planning for the production of orthophotos or photo maps to lay down the parameters to be used for the photoflight and differential rectification. After classification of the known orthoprojection instruments, the parameters of "focal length", "photo scale", "flight data", "end and side lap" as well as "design and time of photoflight", guidelines are developed. As regards rectification, various factors affect the parameters of "scan width" and "scanning speed".*

The starting point of project planning is invariably the product desired, in the present application an orthophoto or photo map. Design data are the map scale and the sheet layout, or the scale and format of the orthophoto, accuracy tolerances and information on the desired image quality that depends on photographic resolution, mismatches and image motion. Other factors affecting the general approach are information on whether the orthophoto is required as a positive or negative, laterally inverted or unreversed, as an end product or only as an intermediate stage. On the basis of these design and product parameters, the parameters to be applied to the photoflight and differential rectification, the project parameters are then selected. First of all, a suitable camera has to be chosen. In view of the standardized 9 × 9-inch format (23 cm × 23 cm), this usually boils down to selecting a suitable camera focal length. The parameter of photo scale (and thus the relationship between the scales of aerial photo and orthophoto) is determined by the service ceiling of the aircraft used. The remaining parameters for the flight planning then are end and side overlap, flight design and time of flight. For differential rectification, the profile interval or scan width and the mean profiling speed to be used by the operator have to be selected.

In the following paragraphs these prime parameters, their interaction and the aspects governing their selection are discussed in order to develop guidelines for project planning. These considerations will be based on the so-called *1 photo equals 1 map* technique, i.e., coverage of a (roughly square) map sheet with one aerial photograph which for this purpose should be differentially rectified, if possible, in a single operation by jointless model connection (e.g., by means of the ZEISS GZ-1 Orthoprojector or an equivalent instrument), because this technique is constantly gaining in importance due to its considerable organizational and economic advantages. In order to allow conclusions to be

*This article describes the results of the author's thesis at Stuttgart University.

drawn as to the degree to which the results obtained apply to all the orthoprojection instruments known, the basic differences between the design and operation of the equipment available on the market are analyzed at the outset.

Principles of Differential Rectification

The operation of the different orthoprojection instruments can be distinguished by mathematical and technical principles. A distinguishing mathematical characteristic is the geometrical element that is rectified at a given instant. Thus, the image may be transformed and reproduced either point by point, in linear form, or in the form of segments. Rigorous point-by-point rectification is not being used up to now. Linear transformation is most widely employed. It is exclusively performed in a continuous manner by lining up adjacent lines in systematically distributed strips, the *strip limits equals line length* being given by the variable width of a scanning aperture. In the scanning direction, the aperture is so narrow that it may be considered as infinitely small (that is, as a line) with respect to the geometry of rectification. If the points imaged in a linear element differ in elevation, only those points will have exact horizontal position whose elevations coincide with those of the model profile used to control the instrument. Points of different elevation on the same linear element deviate from their nominal position by the error inherent in the operating principle.

For rectification over unit areas, regular segments are transformed and reproduced in a discontinuous, back-and-forth scanning pattern. Here also, rectified points whose elevation differs from that of the reference point, are originally affected by the error inherent in the technique. This error can be reduced by additional rectification within the unit of rectification. If this rectification is a linear (affine) transformation in the mathematical sense, we can speak of first-order differential rectification by comparison with zeroth-order differential rectification (without additional rectification). A corresponding higher-order rectification is then also possible for an additional higher-degree transformation.

This defines the second important mathematical classification. In order to facilitate the understanding of these geometrical conditions, we may consider zeroth-order differential rectification within the unit areas as rectification to a horizontal plane, in the case of first-order as rectification to inclined planes and, in the case of higher order, to curved planes (Figure 1). Within the linear element or unit of area, the plane of rectification may, for example, be applied to the ground surface as a tangential plane (called *tangent* in the following) or as a polyhedral surface (called *secant*).

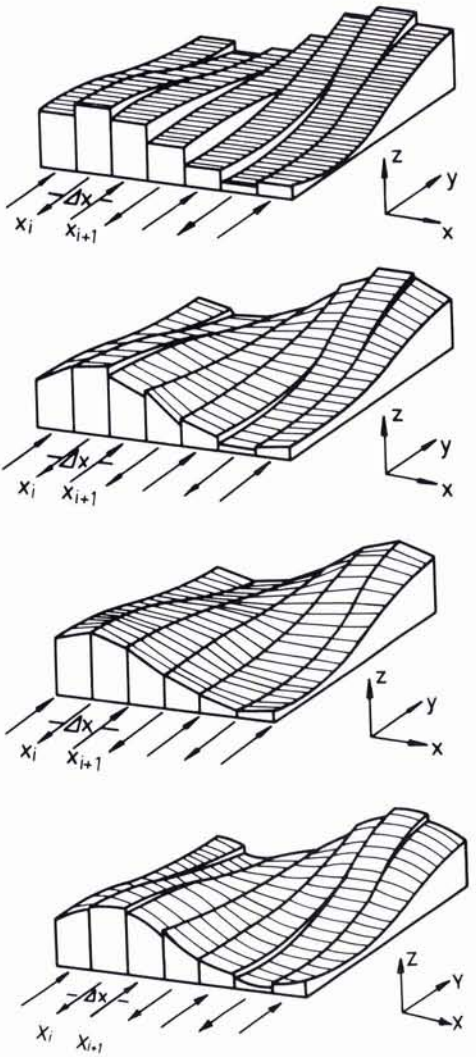

Fig. 1. Model approximation as a function of the degree of differential rectification *From top to bottom:* Zeroth order; First order, "tangent"; First order, "secant"; Higher order, "tangent".

The third possibility of mathematical classification consists in the type of relationship between the photo and the plane of rectification. Here we have to distinguish between central-perspective (geometrical) relationship (represented in the known equipment by the reconstruction of the light path or by affine modification) and functional relationship (image plane and projection surface

TABLE 1. CLASSIFICATION OF KNOWN EQUIPMENT FOR DIFFERENTIAL RECTIFICATION.

Degree of Rectification: Relationship	Element of Rectification	Zeroth order	First order: "Tangent"	First order: "Secant"	Higher order
Central-Perspective Relationship (reconstruction of light path)	Line element (optical transfer)	GZ 1-Orthoprojector ZEISS (on line) Ortho-3-Projector ZEISS Orthophotographe 693 MATRA-SFOM Orthophotographe 910 MATRA-SFOM Orthosfom 9300 MATRA-SFOM Orthophotoscope T 64 KELSH Orthoscan K-320 DANKO FT-Schtsch I USSR		GZ 1-Orthoprojector (off line) + optical ZEISS interpolation	
Functional Relationship (vertical light path)	Line element (optical transfer)	Topocart-Orthophot JENA Orthoprinter OP OMI PPO 8-Orthophoto WILD attachment Orthophoto-Simplex GALILEO			
	Line element (electronic transfer)		B 8-Stereomat WILD-RAYTHEON Stereomat A 2000 WILD-RAYTHEON		
	Area Element (electronic transfer)	UNAMACE BUNKER-RAMO	Analytical Plotter BENDIX AS 11 C		Gestalt Photomapper HOBROUGH GPM

have random orientation, generally vertical light path, correlation between corresponding image and orthophoto points by mathematical functions). Table 1 shows a classification of the equipment for differential rectification presently available on the basis of these mathematical criteria.

The aforementioned possibilities of mathematical classification are supplemented by purely technical differences: optical or electronic imaging, use of one picture of the stereoscopic pair or of a third photo for projection, rectification of a complete photograph by *jointless model connection* or only of the neat stereoscopic model and on-line or off-line control of the differential rectifier. With regard to the following discussion of differential rectification techniques, however, the design criteria with the exception of full-image or partial-image rectification are of no importance. Wherever a distinction between full-image and partial-image rectification or double models and single models is of any consequence, the entire photo size will be used as a basis. This will generally allow suitable conclusions to be drawn for limited areas of a model.

What are the differences between the mathematical criteria for the purpose of orthophoto project planning? By comparison with the parameters applying to linear (continuous) rectification, the extension of the unit area in the scanning direction has to be added for discontinuous imaging. Inasmuch as in all known instruments of the discontinuous type the extension in the scanning direction (generally y) is smaller than the extension at right angles to the scanning direction ($\Delta y < \Delta x$), no separate discussion of Δy seems to be necessary. The selection of scan width Δx or of the area $\Delta x \cdot \Delta y$ depends on the accuracy of model approximation, i.e., of the degree of differential rectification. If model approximation is improved for a specified accuracy, a greater scan width or a larger unit area can be chosen. For discontinuous imaging, no incremental speed need be chosen because this is given by the system and has no effect on the different parameters because it is purely a speed of advance between exposures. For continuous imaging, an exposure is made through the scanning aperture $\Delta x \cdot dy$ during the scanning motion. As for reasons of energy, the extension of the scanning aperture in the scanning direction dy cannot be infinitely small, we have an exposure time of finite magnitude. In other words, we may here encounter a certain displacement of the projected image in relation to the film. This image motion will be examined in conjunction with the selection of an optimum camera focal length.

What are the differences resulting for project design from central-perspective and functional correlation? If in instruments with a vertical light path the effect of φ, ω and κ is compensated by image rotation and extension, image formation is mathematically identical with each of the two principles. In this instance, no difference would affect project design. Contrary to the principle of relationship, the degree of differential rectification has a considerable effect on the selection of project parameters. This refers above all to the accuracy of model approximation so that under identical plotting conditions higher-order differential rectification will reduce unavoidable errors in the orthophoto or, conversely, larger increments of x can be used for a given error tolerance (see "Profile interval . . ." later on).

Selecting the Camera Focal Length

Wide-angle cameras, with which over 80 percent of all mapping photography are obtained today, may be considered as standard cameras for photogrammetric purposes. Due to the almost universal use of the 9 × 9-inch negative size (23 cm × 23 cm), the most widely used focal length is thus 6 inches (153 mm). Wide-angle photography is also used predominantly for the production of orthophotos. On the one hand, this is due to the fact that the majority of orthoprojectors and stereoplotters as well as plotting techniques are designed for wide-angle photography, whereas the other wide-angle photography is available for large areas. This historical trend from normal-angle to wide-angle cameras and the development of ultra-wide-angle lenses during the last decade have been based on the desire to cover as much ground as possible with a single photograph from a given flying height and to obtain higher vertical accuracy due to the resulting more favorable intersection of homologous rays.

Practical experience has shown that the accuracy of differential rectification is essentially determined by the dynamic profiling error of the human operator or the automatic correlator as well as by the error inherent in the technique employed. By comparison, the model errors depending on focal length are negligible. The error dz of model approximation in the profiles (profiling error) and between the profiles (plus errors inherent in the technique) affect the horizontal accuracy according to the formula

$$dr = (r'/f)\, dz = h(r', dz). \qquad (1)$$

If we assume that the errors dz of model approximation in the aerial photo or the orthophoto are about evenly distributed (the profiling errors are correlated with the ground conditions and thus are not normally distributed, but the overall distribution of ground slopes and curvatures in the orthophoto can be considered as uniform), the distribution of the resulting horizontal error can also be determined because the distribution of image radius r' is known (the check points generally have random distribution within the square image area so that the distribution for r' is given by the area as a function of r').

For the distribution of a function $dr = h(r', dz)$ of two random variables r' and dz, we have the distribution function $G(dr)$ where $g(r')$ and $g(dz)$ are the density functions:

$$G(dr) = \iint_{h(r',dz)\leq dr} g(r', dz)\, dr'\, d(dz) = \sum g(r') \left[\sum_{h(r',\,dz)\leq dr} g(dz)\, d(dz)\right] dr' \qquad (2)$$

In this manner, we can determine not only the distribution for dr but also a *mean* value dr_m which will not be exceeded with probability $w = 0.6827$. Writing s' for the side length of the net negative size, the summation approximating integration gives

$$dr_m = \frac{s'}{1.32 \cdot f} \sqrt{(0.6827/\pi)}\; dz_m. \qquad (3)$$

With increasing camera focal length, the effect of profiling errors and inherent errors is reduced proportionately. For the profiling error we can expect approximately $0.003\ dz$, equivalent to about 0.08 to 0.18 mm at the orthophoto scale. With $s' = 180$ mm and a profiling error of 0.15 mm, the effect of the profiling error on horizontal accuracy is then on an average about 0.11 mm for a focal length of 85 mm (3⅓ inches), 0.06 mm for 153 mm (6 inches) and 0.03 mm for 305 mm (12 inches). Although the profiling error thus has a noticeable effect on horizontal accuracy for superwide-angle photography, this error is negligible with a focal length of 153 mm (6 inches). In other words, a focal length of at least 153 mm (6 inches) should be used for differential rectification. For longer focal lengths a higher profiling error and thus a higher profiling speed are admissible.

However, longer focal lengths not only improve horizontal accuracy but also reduce the irregularities occurring in zeroth-order differential rectification at the edges of orthophoto scanning paths due to abrupt level differences in the surface of approximation. These irregualrities introduced by the error inherent in the technique take the form of mismatches (horizontal displacements along the edge of the scanning path) and double images or loss of detail (displacement across scan edges). A special form of double imaging is produced by grazing incidence of the taking ray on the ground surface. In this case, or in the case of even greater ground slope (dead spaces), image detail is generally reproduced several times in adjacent paths (Figures 2 and 3). In the aerial camera, a certain ground surface is reproduced as a point in the photograph; during differential rectification, this

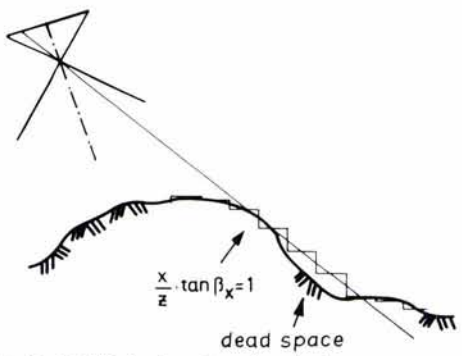

FIG. 2. Multiple imaging for dead spaces $(x/z)\tan\beta_x > 1$.

image point must again be extended to a finite length. If the projection surface is inclined less than would correspond to the actual ground slope, the point and its x-surroundings will be reproduced in several adjacent scanning paths. The longer the focal length, the greater is the ground slope up to which dead spaces and multiple imaging can be avoided.

It is not only the rendition of the ground surface itself but also of high topographic objects that is influenced by the focal length of the aerial camera. In near-vertical photography, off-axis objects are reproduced with central-perspective distortion; in other words, there will be converging verticals. These converging verticals cannot be transformed back into a vertical representation by differential rectification, because this would call for detecting and correcting (electronic) systems which are not yet available. Although rectification thus geometrically produces an approximate parallel projection, the visual impression of central perspective remains unchanged. For high-rise buildings, high vegetation and isolated terrain features

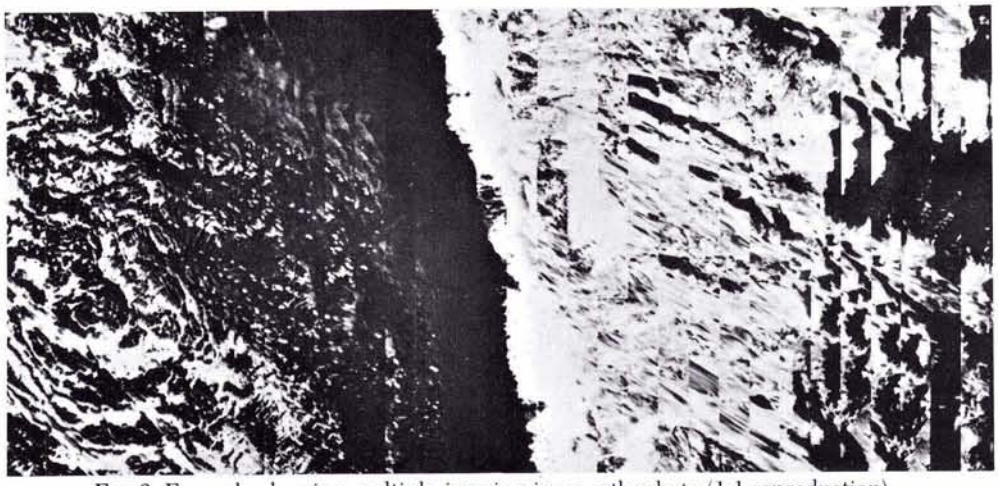

FIG. 3. Example showing multiple imaging in an orthophoto (1:1 reproduction).

for which no allowance can be made during profiling, this will result in converging verticals which will be all the more pronounced, the larger the angular field, that is the smaller the camera focal length. At orthophoto scales $m_{map} \geq 25{,}000$, the converging verticals are of no practical importance, because the objects concerned are too small to show exact detail. At large scales, converging verticals can be very disturbing, above all if several orthophotos or map sheets are assembled into single units, in which the buildings in adjacent sheet corners will be distorted by converging verticals in opposite directions. A comparison made with 1:5,000 scale photography of different focal length taken of the same urban area has shown that for this scale the focal length should at least be $f = 153$ mm (6 inches) or preferably $f = 210$ mm (8¼inches) in order to keep these distortions within tolerable limits.

Image motion in stripwise orthophotos that have been continuously rectified with the aid of linear elements is likewise a principal defect which, among other things, is a function of angular field in the aerial camera. Because the orthophoto is exposed with the scanning aperture in motion, and because for reasons of energy the exposure time cannot be infinitely short (finite extension of aperture in the motion direction), the projected rays may evidence a certain displacement in relation to the film during exposure. Writing b for the extension of the scanning aperture in the motion direction and $tan\ \beta_y$ for the ground slope in the profiling direction, the amount of image motion is

$$s_r = \frac{b\ (r/z)\ tan\ \beta y}{1\text{-}(y/z)\ tan\ \beta y}\ . \qquad (4)$$

Image motion increases with angular field r/z or its projection onto the y,z-plane. This is why it is reduced by small angular fields and long focal lengths. Another possibility of reducing image motion is to use narrower scanning apertures. However, as is evident from Equation 4, the latter trick practically has no effect if the angle between the image-forming rays and the ground surface is very small—$y/z \cdot tan\beta y \approx 1$—as in rough terrain.

In order to determine the tolerable blur introduced by image motion, air photos of different scale and showing different terrain were reproduced by differential rectification onto a plane inclined in the direction of scanning paths so that the amount of image motion could be found theoretically for any point of the orthophoto. These sections were submitted to three different observers who were instructed to assess the admissible amount of blur. According to this test, tolerable image motion varies between 0.4 and 0.8 mm with individual judgement by the observers showing good agreement. For small scales and for photography showing very fine detail, the demands are higher (0.4 mm), for medium and large scales and less pronounced image detail image motion of 0.6 – 0.8 mm is admissible. Assuming 0.5 mm as an admissible tolerance and the widely used scanning aperture of $b = 1$ mm, we can then specify the shortest camera focal length for a certain type of terrain if image motion is to remain below 0.5 mm. If for the different types of terrain we assume the distribution of mean ground slope given by Neubauer, focal lengths of at least $f = 153$ mm (6 inches) should be used for flat terrain, of at least $f = 305$ mm (12 inches) for medium-high mountains and of $f = 610$ mm (24 inches) for high mountains.

For differential rectification aimed at producing photomaps an effort should therefore be made always to use the longest possible camera focal length. However, we shall see that for a certain orthophoto scale and the corresponding initial photo scales to be determined as described in the following section, the necessary flying height will increase accordingly. Increasing flying heights mean higher flight costs so that in practice it will almost always be necessary to adopt a compromise between optimum quality of the results and expenses. Allowance for this problem will therefore have to be made in the following section in connection with determination of the optimum photo scale. As flight costs increase primarily with the type of aircraft required for certain altitudes, we shall, for the time being, take the optimum camera focal length to mean the longest focal length that can still be used within a certain altitude range.

Selecting the Scale Ratios

A very important decision in planning orthophoto projects is the selection of the scale ratios between:

photo : model : orthophoto : map.

In order to avoid having to enlarge the orthophoto with the additional work and possible loss in quality involved, exposure of the orthophoto at the final map scale is highly desirable. If we project the orthophoto at a smaller scale, the area to be exposed will be smaller so that the exposure time is reduced by the square of the scale ratio at identical scanning speed. However, inasmuch as the profile interval and profiling speed to be selected for the accuracy required are a direct function of the final scale, a smaller orthophoto scale calls for higher accuracy, which means that the scan width and the profiling speed in the stereo model should be reduced to the same extent. In other words, practically no time will be gained. On the other hand, the opposite situation of a larger orthophoto scale, as is generally used for better interpretation where orthophotos are employed for revision of medium-scale topographic maps, involves only partly more time. In this instance, the ratio between orthophoto scale and map scale is a design magnitude that is specified in advance and need therefore not be discussed here.

The model scale as an intermediate scale as used in a number of instruments depends practically exclusively on the instrument employed and therefore is likewise of secondary importance for a study of project planning. The question of scale ratios therefore concentrates on selecting the photo scale as a function of the desired orthophoto or map scale. This selection also applies to instruments in which the orthophoto is obtained at an approximate photo scale, because here a suitable enlargement becomes necessary.

The desired image quality and accuracy of the orthophoto, as well as its economical production, are of importance for selection of the scale ratio. The image quality of an orthophoto should be such that it exceeds the resolving power of the human eye at the distance of distinct vision, 8 to 10 inches (20 – 25 cm). Depending on object contrast, the resolving power of the human eye is 2 – 5 minutes of arc, which at the distance of distinct vision is equivalent to about 1.5 – 4 lines/mm (low and high contrast, respectively). For screening orthophotos, the screen used should have 60 to 80 lines/cm. This corresponds to a resolution of 6 to 8 lines/mm so that the orthophoto should have a resolution of about 4 lines/mm for low contrast and 6 lines/mm for high contrast. Although it is true that mapping lenses and aerial film will resolve 60 to 80 lines/mm, the resolution obtained on actual flying missions is not higher than 25 to 30 lines/mm. Assuming imaging according to the expressions:

$$\frac{1}{N^2} = \frac{1}{N_1^2} + \frac{1}{N_2^2} \quad \text{for high contrast}$$

$$\frac{1}{N} = \frac{1}{N_1} + \frac{1}{N_2} \quad \text{for low contrast,} \qquad (5)$$

where N is resolution in lines/mm, the quality of aerial photography is reduced to 18 to 24 lines/mm for good projection lenses (AWAR 60 to 80 lines/mm) and to about 11 to 18 lines/mm with simple projection lenses (AWAR 20 to 30 lines/mm) as referred to the image plane. If this resolution remaining after image formation is related to the specified resolution of 4 to 6 lines/mm, it becomes obvious that a maximum magnification of 4× should not be noticeably exceeded with good projection lenses and of 3× with simple projection lenses. Only if the orthophoto is to be used as background information for a photo map, that is if there is a considerable amount of cartographic treatment, does a lower resolution and thus higher magnification appear admissible.

Magnification may also be limited by the specified horizontal accuracy. Of the factors affecting the horizontal-position error, namely, image errors, model errors, profiling errors, inherent errors, instrumental errors

and cartographic errors, it is primarily the profiling error, as has already been mentioned under 3 which, together with the model error, falsifies the projection distance. According to Equation 3, we obtain for 0.003 z:

$$dr_m = \frac{s'}{1.32 \cdot f}\sqrt{\frac{0.6827}{\pi}}\, dz_m = \frac{s'}{1.32 \cdot f}$$

$$\sqrt{\frac{0.6827}{\pi}}\,\frac{0.3}{1000}\, z, \quad \frac{z}{f} = \frac{1.32 \cdot 1000}{0.3 \cdot s'},$$

$$\sqrt{\frac{0.6827}{\pi}}\, dr_m \approx 52\, dr_m. \qquad (6)$$

Assuming 0.1 mm as the admissible component of the projection-distance error dr_m, we then obtain about $z/f \lesssim 5\times$.

The decisive factors to be taken into account for selecting the photo scale are the maximum flying height, flight tolerances and the flight configuration. In photogrammetric practice, two different flight configurations are generally used:

- It is attempted to cover the largest possible area with a single photograph *(1 photo → max. area coverage)*.
- A single photo is to cover one map sheet which in the following is assumed to be square *(1 photo → 1 map)*.

In selecting the photo scale for the principle of maximum area coverage, the expression originally given by von Gruber for scale m.

$$m_{photo} = c_1 m_{map(c_2)} \qquad (7)$$

is frequently used, in which a value of 0.5 is today assumed for the constant c_2 and of 200 to 250 and more for c_1.

However, if a certain sheet outlay is given, the second method *(1 photo → 1 map)* seems preferable. In this instance, no complex assembly of orthophotos with the need for manual retouching is required. In addition, homogeneous density is achieved throughout the map sheet. Another advantage is that every single map sheet presents a true bird's-eye view because converging verticals are uniformly radial. Also, light and shadow is reproduced uniformly over the entire map sheet. Finally, organization is much easier and economy much greater so that the method *1 photo → 1 map* seems generally desirable for the production of photomap series. Assuming this is true, the ground surface reproduced in a single aerial photograph $(s'\, m_{photo})^2$ must in any instance exceed the required surface area $(s\, m_{map})^2$ in order to make allowance for flight tolerances:

$$s'\, m_{photo} > s\, m_{map}$$

$$\frac{m_{photo}}{m_{map}} > \frac{s}{s'}. \qquad (8)$$

If a single photograph is to cover one complete map sheet, the line of flight should coincide with the straight line joining the map centers. Whenever the aircraft is exactly over the map center on the ground, a photograph should be taken that is as nearly vertical as possible. The deviation between the camera station and the exact map center, the swing and the roll and pitch of the aircraft will result in a certain displacement of the desired map surface in relation to the surface photographed so that a safety margin $\Delta s'$ is required:

$$\frac{m_{photo}}{m_{map}} \geq \frac{s}{s' - 2\Delta s'}. \qquad (9)$$

Figure 4 shows the effect of flight tolerances. The following algebraic relations apply to the figure:

$$s^* = s' / (\cos \kappa + \sin \kappa)$$

$$s'_k/2 = (s'/2) / (\cos \kappa + \sin \kappa) - \Delta y' + t'$$

$$\Delta x' = dx' + f \tan \phi$$

$$w = \Delta y' - \Delta x'$$

$$u = w/(\cos \kappa + \sin \kappa)$$

$$t = u \sin \kappa$$

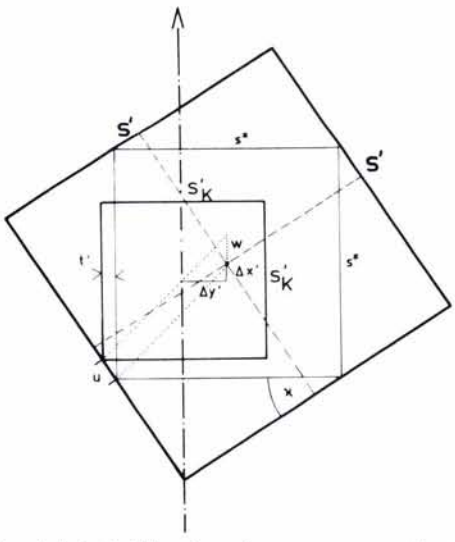

FIG. 4. Admissible size of a square map sheet, making allowance for flight tolerances (at photo scale).

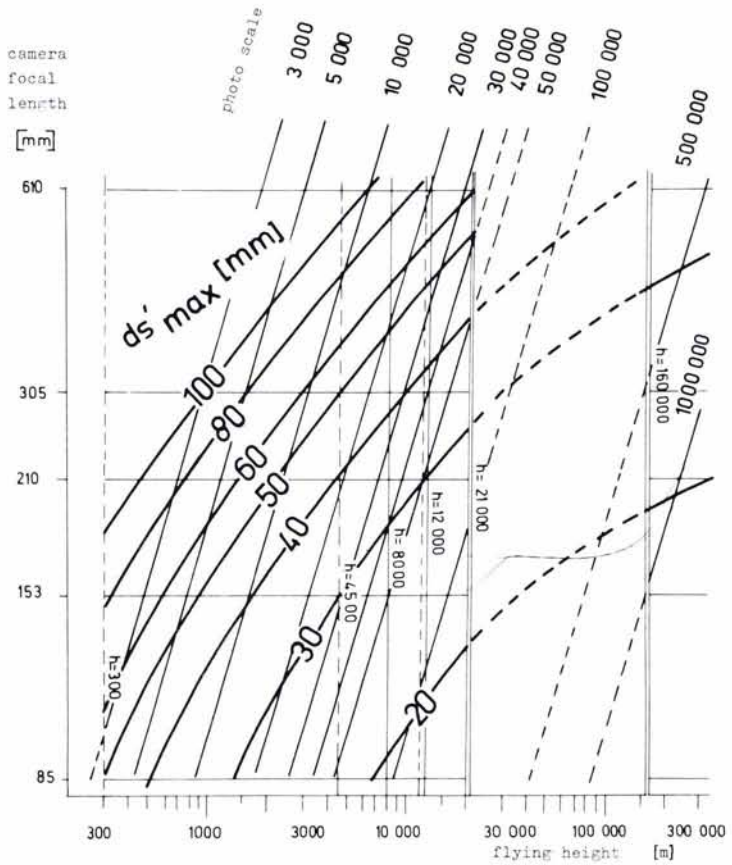

FIG. 5. Maximum deviation from flight path ds'_{max} (or safety margin $\Delta s'_{max}$) as a function of camera focal length, flying height and normally distributed flight tolerance with $\kappa_m = \pm 3^g$, $\omega_m = \pm 1^g$, $dY_m\, m = \pm 3\sqrt{h[m]}$.

$$t' = (\Delta y' - \Delta x')\ sin\ \kappa\ /\ (cos\ \kappa + sin\ \kappa)$$

$$\Delta y' = dy' + f\ tan\ \omega$$

$$s'_k/2 = (s'/2)/(cos\ \kappa + sin\ \kappa) - (dy' + f\ tan\ \omega)$$

$$+ (dy' + f\ tan\ \omega + \Delta x')\ sin\ \kappa/\ (cos\ \kappa + sin\ \kappa).$$

The value s'_k is equal to s_{map} at the photo scale.

If we assume high overlap in the line of flight, only the components κ, dy' and ω acting at right angles to the line of flight will be of importance. If we assume, moreover, that each of the components is normally distributed, we can determine the distribution of the resulting flight-path deviation ds' including average and maximum values on the basis of known statistical averages. According to data used in practice, we may assume $\varphi_m = \omega_m \approx \pm 1^g$, $\kappa_m \approx \pm 3^g$. For the mean deviation of the aircraft at right angles to the line of flight we may assume $dY_m\,[m] = 3\sqrt{h}\,[m]$ or $dy_m'\,[mm] = 3f\,[mm]/\sqrt{h}\,[m]$. As a function of the camera focal length and the flying height, this gives the maximum deviation from the ideal flight path ds'_{max} that will not be exceeded with 99.73 percent probability (Figure 5) or the safety margin $\Delta s'$ to be provided.

We thus also have determined the minimum magnification m_{photo}/m_{map} given in Equation 9, and we can indicate the minimum photo scale to be used for a given map scale (Table 2).

With small-map scales, the method *1 photo → 1 map* results in high flight altitudes which up to now had not always been possible for lack of suitable photographic aircraft. As a result of this restriction which is also reflected in the constants previously used in Equation 7, small-scale map sheets had to be obtained by joining several photogrammetric models. This considerable investment of

TABLE 2. OPTIMUM PHOTO SCALE

	m_{photo} m_{photo}/m_{map} h				
f / m_{map}	85 mm	153 mm	210 mm	305 mm	610 mm
1,000	‡/ 3 900 ‡/ 3.9 ‡/ 330 m	3 700/4 300 3.7/4.3 570/ 660 m	*	*	*
2,500	6,700/ 8,000 2.7/ 3.2 570/ 680 m	7,200/8,300 2.9/3.3 1,100/1,300 m	8,000/9,500 3.2/3.8 1,700/2,000 m	9,000/10,500 3.6/4.2 2,700/ 3,200 m	*
5,000	12,000/14,500 2.4/ 2.9 1,000/ 1,200 m	13,000/15,500 2.6/3.1 2,000/ 2,400 m	13,500/16,500 2.7/3.3 2,800/ 3,500m	15,000/18,000 3.0/3.6 4,600/ 5,500 m	*
10,000	22,000/27,000 2.2/2.7 1,900/ 2,300 m	23,000/29,000 2.3/2.9 3,500/ 4,400 m	25,000/30,000 2.5/3.0 5,200/6,300m	26,000/32,000 2.6/3.2 7,900/9,800 m	34,000/* 3.4/* 20,700/*
25,000	52 000/65 000 2.1/2.6 4 400/ 5 500 m	55,000/65,000 2.2/2.6 8,400/ 9,900 m	55,000/70,000 2.2/2.8 11,500/14,700m	†	†
50,000	105,000/130,000 2.1/2.6 9,000/ 11,000m	110,000/130,000 2.2/2.6 16,800/ 20,000m	†	†	†
100,000	200,000/250,000 2.0/2.5 17,000/ 21,000m	†	†	†	260,000/320,000 2.6/3.2 158,000/195,000 m

*: $v \gtrsim 4x$
†: $21{,}000 \lesssim h \lesssim 160{,}000$ m
‡: $h \lesssim 300$ m.

orientation and plotting can be avoided by the method *1 photo → 1 map* if high-altitude flights are used. However, the saving in the plotting stage is offset by higher flight costs. Photoflight organizations give a relation of approximately 1 : 2 : 5 for the costs of simple piston-engined aircraft ($h \gtrsim 4{,}500$ m/15,000 ft), in relation to high-powered piston-engined aircraft ($h \gtrsim 8{,}000$ m/27,000 ft) and jet aircraft ($h \lesssim 12{,}000$ m/40,000 ft). Even greater altitudes are reached by special-purpose aircraft (e.g., U2 with $h \lesssim 21{,}000$ m/70,000 ft) which only recently have become available for civil use. It is, of course, very difficult to quote a cost factor for this particular situation. We have to assume that the military of the country concerned owns and maintains the aircraft and will only charge actual operating costs. For this we may assume a cost factor of ten times the one for simple piston-engined aircraft. In the future, satellite photography taken from heights of 160 km and more may become possible for civil purposes.

The economy of high-altitude flights for medium and small-scale photo maps will be shown by the following example: for a 1 : 100,000 scale photo map of the type under discussion for relatively feature-less areas, a photo scale of $m_{photo} = 94{,}000$ can be obtained with an super-wide-angle camera and a high-powered piston-engined aircraft (h = 8,000 m/27,000 ft). According to Figure 5, the useful net photo size is $s' = 190$ mm so that double-model plotting will cover a map area of $s^2 = 180 \times 180$ mm². A 500 × 500 mm² map sheet would have to be covered by nine double models.

If a U2 aircraft (h = 21,000 m/70,000 ft) is available, for example, $m_{photo} = 250{,}000$ with $s' = 200$ mm can be obtained with super-wide-angle photographs. The orthophoto

surface is $s^2 = 500 \times 500$ mm^2 so that a complete map sheet can be covered by a double model. Although according to the previous assumption the flight costs are five times higher, the plotting costs are reduced to $^1/_9$. This saving is all the more important because compared with flight costs, the plotting costs are the greater part of the costs of a double model. In addition, there is a certain saving due to the elimination of mosaic work and the far lesser control density. Under these circumstances, the smaller number of suitable flight days due to the higher altitude is acceptable.

If allowance is made for the demand that the camera focal length should be as long as possible and the flying height as low as possible as well as for the effect which the requirements regarding image quality and accuracy have on scale, an optimum photo scale can be chosen in accordance with the results shown in Table 2. Whether the desired optimum magnification from photo to orthophoto can be obtained directly depends entirely on the magnification range of the orthoprojection instrument available. As the actual photo scale varies in accordance with the ground relief, the magnification range that can actually be used for project planning is smaller than indicated by instrument manufacturers. In some instruments, there are additional restrictions, for example, due to photo tilt.

Flight Design

Once the camera focal length and the desired photo scale have been selected, the nominal flight height should be chosen with due allowance made for the equipment operating ranges, the ground relief and the usual variations of flying height. In order to make sure that the safety margin $\Delta s'$ will be sufficient even in the most unfavorable application (mountain at edge of map sheet, see Figure 6), the flying height h_G given by $f \cdot m_{photo}$ should be referred to the peaks H_{max}:

$$\begin{aligned} h_{peak} &= f\, m_{photo} \\ h_{valley} &= f\, m_{photo} + \Delta H \\ h_{sea} &= f\, m_{photo} + H_{max}. \end{aligned} \tag{10}$$

If $\pm\, h_T$ is the vertical tolerance allowed for the flight path, the minimum flying height to be maintained is then

$$h_{sea} = f\, m_{photo} + H_{max} + h_T. \tag{11}$$

The z-range of the orthoprojector is sufficient if

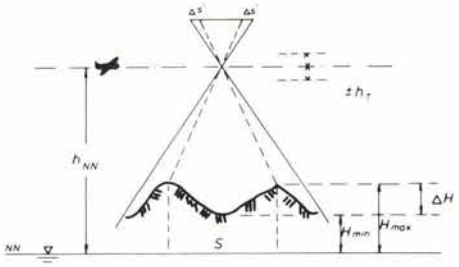

FIG. 6. Flying height and ground relief.

$$z_{min} < \frac{h_{min}}{m_{map}} = \frac{f\, m_{photo}}{m_{map}}$$

$$z_{max} > \frac{h_{max}}{m_{map}} = \frac{f\, m_{photo} + \Delta H + 2 \cdot h_T}{m_{map}}. \tag{12}$$

In the method *1 photo → 1 map*, the end lap

$$p_{percent} = \frac{s' - b'}{s'} \cdot 100$$

$$= \left(1 - \frac{B}{s' \cdot m_{photo}}\right) \cdot 100 \tag{13}$$

is given by triggering a photo right above the map centers ($B = S_x$). If models have to be formed, at least an intermediate photo is required ($B = S_x/2$). In view of the flight tolerances to be allowed ($S_x = (s' - 2\Delta s') \cdot m_{photo}$), we then have:

without model formation ($B = S_x$):

$$p_{percent} = \frac{2\Delta s'}{s'} 100$$

with model formation ($B = S_x/2$):

$$p_{percent} = 50 + \frac{\Delta s'}{s'} 100. \tag{14}$$

With $B = S_y$ and a square map sheet, the side lap results from

$$q_{percent} = \frac{2\Delta s'}{s'} \cdot 100. \tag{15}$$

Although in the normally used method *1 photo → max. area coverage* the end and side overlaps are parameters that have to be chosen independently, if *1 photo → 1 map* they result as secondary magnitudes as a function of the requirement that a constant base B be available in the terrain. Due to the ground relief (variable photo scale), this base is not constant in the photography so that end lap also varies according to Equation 13. In other words, if it were desired to obtain pin-point

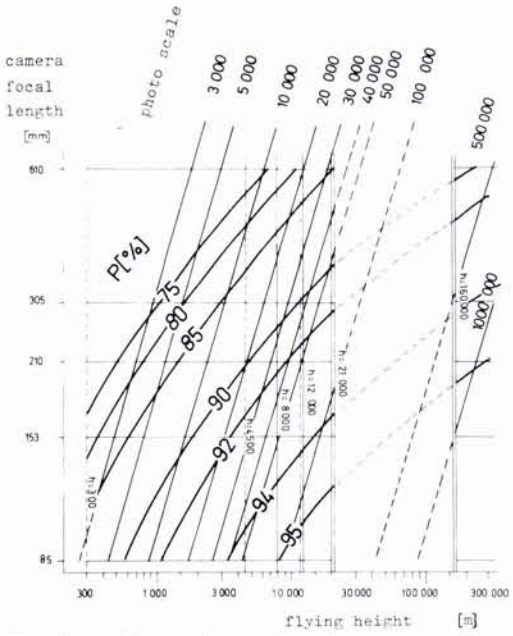

FIG. 7. End lap p (percent) with automatically controlled exposure cycles (random start and no correction of overlap control) as a function of camera focal length and flying height.

photography by precise overlap control, the end lap to be set on the intervalometer would have to be continually varied to make allowance for ground relief. However, this is hardly possible in actual flight practice, just as the manual triggering of photography and visual aiming.

If the desired exposure intervals cannot be obtained otherwise (one possibility would be, for example, to trigger exposures at constant path intervals with controlled air speed), a logical solution will be to try to avoid the necessity of pin-point photography by using a high end-lap ratio. What is the end-lap ratio required to achieve this aim? It can be shown that any desired map sheet will be covered by at least one photograph with a probability of 99.87 percent if

$$b' \leq (2 - \sqrt{2}) \cdot \Delta s' = 0.59 \cdot \Delta s'.$$

We then have

$$p_{percent} \geq \left(1 - \frac{0.59 \cdot \Delta s'}{s'}\right) \cdot 100 \qquad (16)$$

Figure 7 shows the required end lap as a function of camera focal length and flying height. If, in addition, the maximum net photo size in the line of flight is not fully used in determining the final photo scale, the admissible base b' increases as follows:

$$b' \leq 0.59\ \Delta s' + \left(s' - 2\Delta s' - \frac{S_x}{m_{photo}}\right)$$

$$b' \leq s' - \frac{S_x}{m_{photo}} - 1.41\ \Delta s'.$$

Thus, end lap for automatically triggered photography is always at least

$$p_{percent} \geq p_{peak} = \left(\frac{S_x f}{s' h_{peak}} + 1.41\,\frac{\Delta s'}{s'}\right) 100. \qquad (17)$$

In practical flight design we have to check whether at the end lap chosen the desired exposure interval can be obtained with the camera equipment available. A rough estimation shows that, with the exception of satellite photography, the high overlap ratio required for automatically triggered photos can always be attained if the minimum cycling time is 1.5 or 2 seconds. For satellite photography, on the other hand, precise attitude control and thus pin-point photography are possible.

The question of the flight direction to be chosen (east-west or north-south) may be influenced by the side ratio of the map sheets desired. It appears reasonable always to fly parallel to the short sides of the sheet and use single models. A square map format, on the other hand, offers the advantage that full use can be made of the method of plotting double models and that the flight direction can be chosen freely. Another important point may be a systematic orientation of fall lines in the terrain. Here, it is advisable to fly in the direction of the principal fall lines so that the operator during profiling will have to cope with only minor level differences in the different profiles (in practically all instruments for differential rectification, scanning profiles are arranged at right angles to the instrument base).

Contrary to general practice for stereoplotting, the time immediately after trees have come into leaf should be chosen for flying in areas with a vegetation cover. This will improve the legibility of photo maps. Roads and buildings covered up by vegetation can be made visible by subsequent cartographic treatment. In the northern hemisphere, photography should be flown in the afternoon to secure the modeling effect of sunlight at a suitable angle. This applies above all to arid regions where the lack of topographic detail makes the modeling effect of light and shadow one of the primary factors affecting the information content of photo maps.

Profile Interval and Scan Width

The one parameter that is most important for plotting is the increment of X. We here have to distinguish between the profile interval and the scan width, provided that the model scale is different from the scale of the orthophoto. In the ZEISS GZ-1 Orthoprojector, for example, we also have the possibility of increasing the number of exposure scans over the number of model profiles. This allows better model approximation in the off-line mode without any increase in manual or automatic profiling. In the following, the parameter "scan width in orthophoto Δx_{map}" is studied. For a certain practical application, we then obtain the profile interval Δx_{model} as:

$$\Delta x_{model} = \frac{m_{map}}{m_{model}} \cdot \Delta x_{map} \cdot \frac{1}{INT} \quad (18)$$

where INT is the number of model profiles in relation to the number of exposure scans if interpolation of profiles is possible during projection.

In discussing the optimum scan width we have to distinguish between factors that exert their influence and others that are actually decisive. The former are the configuration of the terrain, the principle of rectification employed, the camera focal length and the orthophoto scale. The latter are factors such as the required horizontal accuracy, admissible irregularities at the scan edges and, possibly, the accuracy of simultaneous contour plotting and the aspect of economy.

In differential rectification it is generally desirable to use the greatest possible scan width so that the time required for projection and thus the overall machine time can be kept to a minimum to reduce costs and increase the production rate. It is thus possible, for example, to give the overall machine time required for the production of a double orthophoto of 540 × 540 mm² gross size in the on-line mode as a function of scan width and mean profiling speed. As a fixed share for orientation and all incidental work on the instrument, four hours have been assumed for an orthophoto derived from two models. It is evident, for instance, that an increase in scan width from 8 mm to 16 mm at a speed of 10 mm/sec will reduce the overall machine time only from 5.1 to 4.5 hours, i.e., by 12 percent. If we also take into account that the costs of photogrammetric plotting in the case of the *1 photo → 1 map* technique are only about one quarter the total production cost of an orthophoto map, the resulting gain is only about 3 percent of the overall cost and thus of no practical importance. In other words, scan widths exceeding 8 mm are not interesting. Conversely, scan width of less than 2 mm result in an undue extension of profiling time for the operator so that in difficult terrain somewhat higher errors and greater irregularities will generally be tolerated.

In order to show the interaction between scan width on the one hand and accuracy as well as irregularities in the orthophoto on the other, differential rectification has been numerically simulated. In order to obtain the characteristic profiles required for simulation, nine typical stereo models were selected from existing photographic material. In each of these models, two y-profiles intersecting the nadir points of the photos were scanned in a ZEISS D-2 PLANIMAT and ECOMAT-11 with DTM-1 with a speed of 1.0—1.2 mm/sec, recording intervals of 0.4 and 0.6 mm and a z-resolution of 0.01 mm (in the model) (Figure 8). In order to classify the profiles, mean profile slopes $tan\ \beta_{y\,m}$ and mean relief ΔH_m were computed for every profile by means of Equations 19:

$$tan\ \beta_{y\,(i)} = \frac{z_{i+1} - z}{y}\ ;\quad tan\ \beta_{y\,m} = \frac{\sum tan^2\beta_{y\,(i)}}{n}\ ;\quad z_m = \frac{\sum z_i}{n}\ ;\quad \Delta z_m = \frac{\sum (z_i - z_m)^2}{n}\ ;\quad \Delta H_m = \Delta z_m\, m_{model.} \quad (19)$$

These data define the position of every profile in a $\Delta H_m/tan\ \beta_{y\,m}$-diagram (Figure 9). The profiles were classified as shown in Table 3. Figure 9 shows that one model (arid stratification in Western Persia) should come under hills according to the ground slope, whereas its relief would include it among the flat terrain. In the following, the nine profile pairs measured have therefore been grouped in five types which, contrary to the above terrain classes, might be combined under the following headings: *plains/flat terrain, flat terrain/hills, hills, arid medium-high mountains* and *high mountains.*

In differential rectification with the aid of linear elements we may consider rectification in the scanning direction as continuous. This means that for simulation only the approximation of the model within the linear element in adjacent scans is of interest. The different types of profile measured were therefore considered as profiles across the scanning direction and approximated by the rectification principles defined in the following:

- *O* Projection onto a horizontal surface on the basis of the profile in the center of the

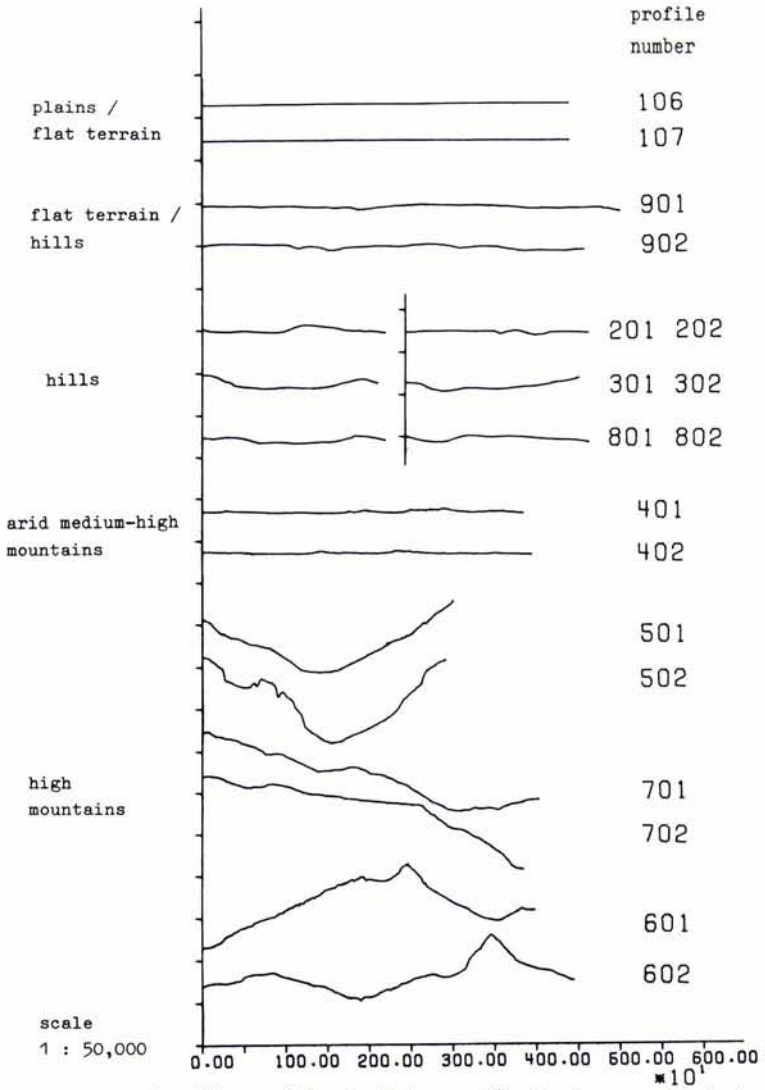

FIG. 8. Ground profiles used for simulating rectification (no exaggeration).

TABLE 3. CLASSIFICATION OF SCANNING PROFILES.

	$\tan \beta_{y\,m}$	ΔH_m
Plains	<0.03	<5 m
Flat terrain	0.03—0.15	5—20 m (20)
Hills	0.15—0.40	20—100 m
High mountains	>0.40	>100 m

scanning path (zeroth order differential rectification).

1 T a The elevation of the profile in the center of the scanning path and the tangent at this point are used as a basis for the profile height and the transverse slope in the scanning path (first-order differential rectification).

1 T b The average elevation and average transverse slope in the scanning path are used as a basis (first-order differential rectification).

1 S 25 Projection onto an inclined plane defined by profiles along the edges of the scanning path (secant), slope being limited to ± 25° (first-order differential rectification).

1 S 35 Secant approximation limited to ± 35° (first-order differential rectification).

1 S Secant approximation with unlimited slope (first-order differential rectification).

2 Rectification to a second-order surface given by three profiles in the center and at the edges of the scanning path (second-order differential rectification.

Each of these rectification principles was then successively used for numerical approx-

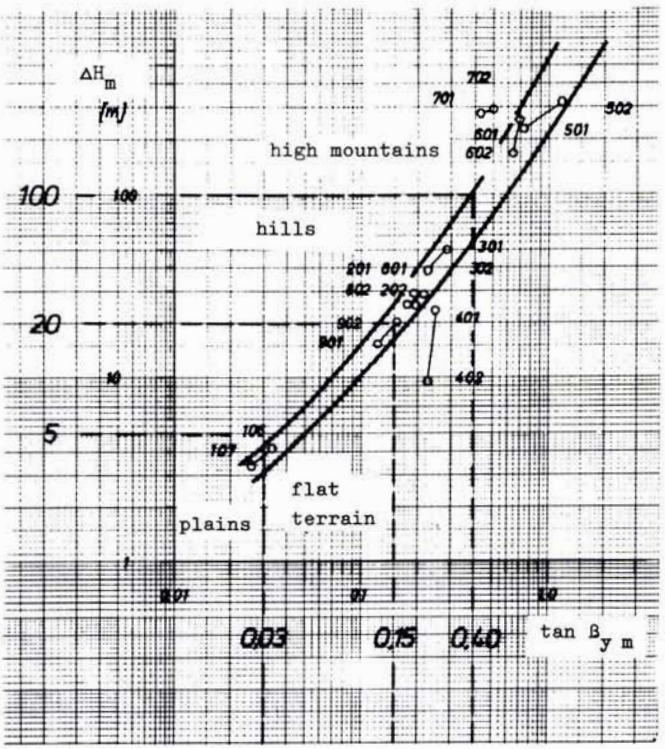

FIG. 9. Comparison of profiles used on the basis of mean relief and mean ground slope.

imation of the 18 profiles with different increments covering 2^n ($n = 2 \ldots 9$ or 10) recording intervals used for computation. In each of these simulations, the differences between profile elevation and the height of the line of approximation were computed, squared and added. As a result, about 1,100 simulations with the corresponding number of mean-square vertical errors of the model approximation were obtained. The results of all the profiles of one group were averaged and the values for the different principles were combined to allow deduction of functions for the vertical error as a function of the increment, introduced by the technique. These $[\Delta H = F(\Delta X)]$-functions are predominantly logarithmically linear. For the profile groups *flat terrain/hills, hills* and *high mountains,* the slope of the curve is about 1 for all rectification principles, i.e., the mean vertical error of model approximation increases in proportion with the increment used. For the profile groups *plains/flat terrain* and *arid medium-high mountains,* the curve slope is < 1, i.e., the increment of X may, for instance, be more than doubled if the specified accuracy tolerance of model approximation is doubled. If very high vertical errors are admissible, the increment will also increase out of proportion, because the boundary case $\Delta X \rightarrow \infty$ does not lead to infinitely large level differences but to the maximum relief of the profile type concerned.

The $[\Delta H = F(\Delta X)]$-functions allow the proper increment of X to be given for any desired accuracy of model approximation, for the type of terrain and the rectification principle concerned. The accuracy of model approximation to be maintained can be determined by Equation 3 as a function of the required mean-square horizontal point error in the orthophoto:

$$\Delta H_m[m] = 1.32 \sqrt{\frac{\pi}{0.6827}} \cdot \frac{f}{s'} \cdot \frac{m_{map}}{1000} \cdot \Delta r_m\,[mm]. \tag{21}$$

A frequently specified map accuracy is 0.2 to 0.3 mm with a 68.27-percent level, or 0.3 to 0.5 mm with a 90-percent level. For the remaining errors such as model errors, profiling errors, instrumental errors and cartographic errors, let us assume 0.16 mm so that 0.2 mm will generally be admissible for the effect of

TABLE 4. ADMISSIBLE SCAN WIDTH (Δx_{map} [mm]) FOR A MODEL-APPROXIMATION TOLERANCE OF $\Delta H_m = \pm$ 2.4 m. (">500" = no limitation; single-step rectification possible)

Type of Profile	Principle of Differential Rectification						
	O	1 T a	1 T b	1 S 25	1 S 35	1 S	2
Plains/ flat terrain	381	62	>500	>500	>500	>500	>500
Flat terrain/ hills	13	19	39	27	27	27	51
Hills	9	14	34	22	22	22	41
Arid medium-high mountains	10	9	26	15	15	15	26
High mountains	2	5	5	2	3	5	11

the vertical error of model approximation (error inherent in the technique used). For the most frequent practical application of $f = 153$ mm/$m_{map} = 5{,}000$ feet ($\Delta H_m = 2.4$ m), the increments given in Table 4 will then result as a function of profile type and rectification principle for a net photo size with $s' = 180$ mm. It is obvious that, with the exception of high mountains, the admissible increments are clearly above the slits generally employed, that is, the required accuracy has hardly any effect on scan width. The following holds for other plotting configurations: according to Equation 21, the tolerable vertical error ΔH_m [m] of model approximation, and thus the admissible increment ΔX [m] increases with longer camera focal length, smaller orthophoto scale and lesser requirements of horizontal accuracy. Where the curve slope is less than 1, this increase is even higher than proportional.

Another factor determining the selection of scan width is the admissible irregularities. For this reason, during model simulation the vertical mismatches at the scan edges including their averages were also determined for those rectification principles in which such irregularities can occur (i.e., for all methods except *1 S* and *2*). The resulting functions show: for the principles *0, 1 T a* and *1 T b* the relationship is about logarithmically linear with respect to vertical accuracy. In very rugged terrain, zeroth-order differential rectification reveals the greatest irregularities, because in practically all applications of $\beta_x \neq O$ there is a vertical mismatch which becomes greater with increasing increment. For first-order differential rectification with model approximation by secants and limitation of slope, there are practically no vertical mismatches at the scan edges except in hills and high mountains, because the actual ground slope exceeds the limiting values of 25° or 35° only rarely. In addition, any larger transverse slope in the scanning path will remain below 25° or 35° due to the finite vertical extension of the ground with increasing increment, as a result of which mismatches are eliminated. In high mountains, each of the different principles exhibits irregularities increasing with greater increment. If in an orthophoto the horizontal irregularities should not exceed an average of 0.2 mm, the criterion of the horizontal-position error according to Equation 21 is applicable here also. Where $f = 153$ mm/$m_{map} = 5{,}000$, the scan width given in Table 5 is admissible. The dependence on the principle of rectification is here more

TABLE 5. ADMISSIBLE SCAN WIDTH FOR A TOLERANCE OF MEDIUM VERTICAL MISMATCHES AT THE SCAN EDGES OF $\Delta H_m = \pm$ 2.4 m (">500" ≙ unlimited).

Type of Profile	Principle of Differential Rectification				
	0	1 T a	1 T b	1 S 25	1 S 35
Plains/ Flat terrain	>102	23	>410	>500	>500
Flat terrain/ Hills	4	8	23	>500	>500
Hills	2	6	20	>500	>500
Arid medium-High mountains	2	4	14	>500	>500
High mountains	0.6	2	1.3	1.0	1.2

TABLE 6. ADMISSIBLE SCAN WIDTH Δx_{map} [mm] FOR A MEAN MODEL-APPROXIMATION TOLERANCE OF $\Delta h_m = \pm 0.1$ mm AT THE ORTHOPHOTO SCALE.

Type of Profile	Principle of Differential Rectification	
	1 S	2
Plains/ Flat terrain	26	51
Flat terrain/ Hills	5	9
Hills	4	9
Arid medium-High mountains	2	4
High mountains	1	2

pronounced than for the horizontal accuracy. Although on the one hand the principles *O* and *1 T a* call for increments of usual magnitude which are thus limited, the secant principles no longer cause any noticeable mismatches (except in high mountains) in spite of the limitation of slope. According to Equation 21, the admissible mean vertical mismatch for other plotting configurations increases with longer camera focal length, smaller orthophoto scale and larger tolerance of mismatches, but due to the predominant curve slope < 1 the admissible scan width increases more than proportionately.

Numerous orthoprojection instruments allow a contour plot to be obtained as a by-product simultaneously with the orthophoto. The outputs are dropped lines for zeroth-order differential rectification, tangent sections for first-order differential rectification with tangential model approximation, and approximate contour lines for first-order differential rectification with model approximation by secants. As contours derived from dropped lines and tangent sections are obtained by manual, graphical construction, only the production of approximate contours in the HLZ Electronic Contourliner by ZEISS can be described exactly mathematically. Only for this application (principle *1 S*) can admissible scan widths therefore be given. It can be shown that for the production of contours from profiles a mean vertical error of ± 0.10 mm at the map scale is still admissible for the inherent error (model approximation). By means of the plotting scale it is thus possible to indicate the scan width as a function of profile type for all focal lengths and plotting scales. Table 6 also shows the values for approximate contours obtained by second-order differential rectification, which are theoretically possible. Here also it becomes apparent that the second-order principle scarcely offers any practical advantage because the number of profiles needed is the same and thus only the time required for automatic projection is reduced to 50 percent.

PROFILING SPEED

Apart from the speed range that is an instrument characteristic, the selection of the profiling speed is determined by the desired profiling accuracy and by economic considerations. The lower the speed, the more accurately is the nominal profile approximated,

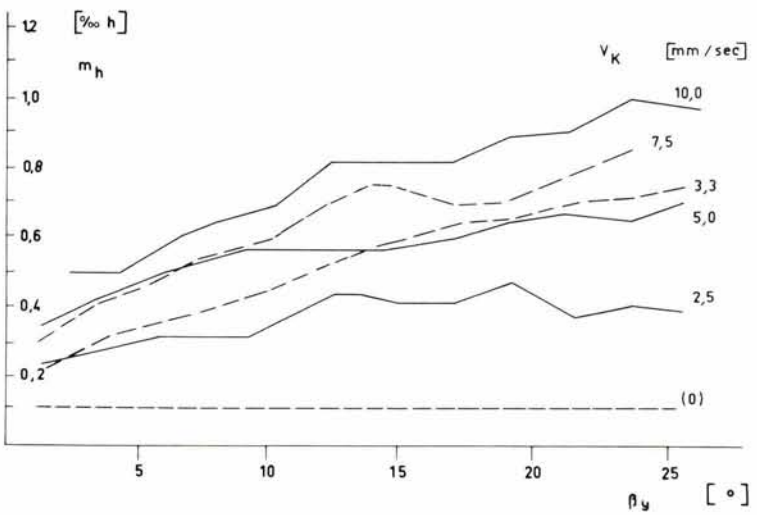

FIG. 10. Mean vertical profiling error as a function of profiling speed and ground slope (averages by Neubauer and Schneider).

the longer the machine time required and thus the higher the costs of an orthophoto. Many workers have already investigated the accuracy of contour plotting as a function of speed. The two most important works are by Neubauer and Schneider and both are considering the dependence on profiling speed and profile slope (Figure 10). The profiling error undoubtedly is a function of ground slope, but this dependence diminishes with diminishing speed and is finally lost completely as the boundary case of static measurement is reached. A dependence on speed becomes noticeable only for larger speed variations. If this result is to be used to formulate a recommendation for optimum speed, it may be said that the best vertical profiling accuracy of 0.3 to 0.4 per thousand of the flight height or projection distance can be expected at the lowest speed (2.5 mm/sec as referred to the orthophoto).

In flat terrain, the same accuracy can also be achieved with higher speed. In selecting an appropriate speed, it is less the ground slope that has to be taken into account than the curvature in the model. In instruments allowing an incremental speed setting, about 7.5—10 mm/sec in practice should be used for flat terrain, 3.3 to 5 mm/sec for hills and 2.5 to 3.3 mm/sec for high mountains. No exact numerical data can be given for instruments in which the speed can be varied during profiling because the operator will always select the speed that he thinks is most suitable. In this instance, it is only necessary to check the operator's subjective judgement by trial runs in order to ensure that it is as nearly objective as possible. If only planimetry is plotted, we are interested only in the horizontal displacement introduced by the profiling error. In this case, a lesser accuracy, i.e. higher speed and lesser attention, is admissible for the central area of the projected image. This point is of particular importance for the plotting of difficult models which demand the operator's full attention (in this case only in the marginal areas).

Reference

1. Hobbie, D.: "Zur Verfahrensdisposition bei differentieller Entzerrung von photogrammetrischen Luftbildern," *Deutsche Geodätische Kommission*, Series C (in press). (Includes further references).

S 51-579-e Printed in U.S.A. V . . . /74 Voo

ISP Symposiums in 1974

The International Society of Photogrammetry is sponsoring a symposium in each of its seven technical Commissions during 1974. Also a joint meeting of the ISP Council and the Commission Presidents will convene in Paris in conjunction with the symposium of Commission IV to finalize the plans for the next ISP Congress to be held in Helsinki July 11-24, 1976.

The ISP Council held its 1973 meeting at ITC, Enschede, the Netherlands, the last of August 1973. (See pages 683, 684 and 762 of the July Yearbook issue of *Photogrammetric Engineering* for additional information about ISP.)

Com. I. *Primary Data Acquisition*. Aug. 27-29. Sec.: Mr. Bengt Adolfsson, The National Road Administration, Fack S-102 20 Stockholm, Sweden.

Com. II. *Instrumentation for Data Reduction*. Oct. 2-4. Sec.: Prof. Bruno Astori, Istituto di Topografia, Politecnico di Torino, Corso Duca dagli Abruzzi 24, I. 10 129 Torino, Italy.

Com. III. *Mathematical Analysis of Data*. Sept. 2-6. Pres.: Prof. Dr. F. Ackermann, Univ. Stuttgart, Institut fur Photogrammetrie, Keplerstrasse 11, D7000 Stuttgart, 1 West Ger.

Com. IV. *Topographic and Cartographic Applications*. Sept. 24-26. Sec.: M. Jean Denegre, IGN, 2 Avenue Pasteur, F 94160 Saint Mande (Paris), France.

Com. V. *Non-Topographic Photogrammetry*. Sept. 10-13. Sec.: Dr. R. E. Herron, Baylor College of Medicine, a333 Moursund Ave., Box 20095, Houston, Texas 77025. Symposium to be held in Washington, D. C., in conjunction with the International Federation of Surveyors (FIG).

Com. VI. *Economic, Professional and Educational Aspects of Photogrammetry*. Sept. 18-20. Sec.: Dr. Ing. Adam. Linsenbarth, Stowarzyzenie Geodetov Polskich, P.O. Box 903, Czackiego 3/5, Warsaw, Poland.

Com. VII. *Interpretation of Data*. Oct. 7-11. Sec.: Dr. A. H. Aldred, Canadian Forestry Service, Dept. of the Environment, 396 Cooper Street, Ottawa K1A OH3, Canada. Symposium to convene in Banff, Alberta, Canada.